January 2001 • NREL/CP/520-29641

Conference Paper

The Deposition and Characterization of Mo/CuInGaSe$_2$/CdS/ZnO Solar Cells

Preprint

H.A. Al-Thani, F.S. Hasoon, J.L. Alleman, and M.M. Al-Jassim
National Renewable Energy Laboratory

D.L. Williamson
Colorado School of Mines

To be presented at the Sharjah Solar Energy Conference
Sharjah, UAE
February 18-21, 2001

National Renewable Energy Laboratory

1617 Cole Boulevard
Golden, Colorado 80401-3393

NREL is a U.S. Department of Energy Laboratory
Operated by Midwest Research Institute • Battelle • Bechtel

Contract No. DE-AC36-99-GO10337

The Deposition and Characterization of Mo/CuInGaSe$_2$/CdS/ZnO Solar Cells

Hamda A. Al-Thani,[a,*] Falah S. Hasoon,[a] Jeff L. Alleman,[a]
Mowafak M. Al-Jassim,[a] and Don L. Williamson[b]

[a]National Renewable Energy Laboratory, Golden, CO 80401, USA
[b]Colorado School of Mines, Phys. Dept., Golden, CO 80401, USA

Abstract

Mo thin films were deposited on sodalime glass (SLG) substrates using direct-current planar magnetron sputtering, with a sputtering power density of 1.18 W/cm^2. The working gas (Ar) pressure was varied from 0.6 mtorr to 16 mtorr to gain a better understanding of the effect of sputtering pressure on the morphology and microstructure of the Mo. Thin films of Cu(In,Ga)Se$_2$ (CIGS) were deposited on the Mo-coated glass using the 3-stage coevaporation process. The morphology of both the Mo-coated SLG and the CIGS thin films grown on it was examined using high-resolution scanning electron microscopy. The film microstructure, such as the preferred orientation, and the residual intrinsic stress were examined by X-ray diffraction.

Keywords: Mo; Cu(In,Ga)Se$_2$; CIGS; 3-stage process; Intrinsic stress; Microstructure

Introduction

Molybdenum is one of the most important materials used as a back ohmic contact for thin-film solar cells. There is a high demand for using this material for Cu(In,Ga)Se$_2$ (CIGS) film growth, because of its high melting temperature and its low resistivity [1]. There is a strong correlation between the energy of the sputtered Mo particles and the working gas sputtering pressure, discharge voltage, and the mass ratio of target and projectile atoms. As a result, significant changes in the properties of the growing films may be induced. The films experience compressive stress with dense microstructure at relatively low pressure due to the high kinetic energy of the arriving atoms. When less energy is provided to the film at relatively high sputtering pressures, films exhibit tensile stress with open porous microstructure [2,3,4]. One mechanism for compressive stress is that due to lattice expansion in the growing films induced by energetic incorporated working Ar gas that bombards the growing Mo films by means of atomic peening action [5, 6].

* Corresponding author.
Tel.: + 1-303-384-6562.
Fax: +1-303-384-6430.
E-mail address: hamda_althani@nrel.gov.

Thin-film CIGS is one of the most promising materials for thin-film photovoltaic devices. This is largely due to the possibility of preparing it in either n- or p-type form, its high absorption constant (3–6 $\times 10^5$ cm^{-1}) for the solar spectrum, and the excellent stability under operating conditions [7]. It also has a desirable variable direct bandgap from 1.02 eV to 1.68 eV, depending on the x = Ga/(Ga+In) ratio [8]. Unacceptable device performance had been reported for the photovoltaic structure with high Ga content ($x > 0.3 - 0.4$)[9]. However, a thin-film conversion efficiency of 18.8% has been achieved with CIGS solar cells [10].

The purpose of this work is to study the effect of the sputtering pressure, at fixed power density, on the morphology and microstructure on the Mo thin films, as well as the subsequently deposited CIGS absorber films.

Experimental

Mo films of thickness 0.6–0.7 μm were deposited on 10.16 cm × 10.16 cm sodalime glass (SLG) substrates by (DC) planar magnetron sputtering. The cathode electrode (Mo target) was 12.7 cm × 20.32 cm × 0.32 cm, with a distance of 75 mm from the SLG substrates. Prior to deposition, the vacuum base pressure was less than 4×10^{-7} torr. To understand the effect of different sputtering partial pressures on the morphology and microstructure of the Mo, the sputtering process was operated in the working Ar gas pressure in the 0.6–16 mtorr range. The average sputtering power density of 1.18 W/cm^2 was used with a discharge current of 1 A and a discharge voltage in the 290–320 V range. The deposition rate was within the average of 11 Å/s. The substrate temperature was difficult to maintain at constant temperature during the deposition; it was increasing gradually from room temperature to about 400 K. CIGS thin films were deposited on the Mo-coated SLG by the "3-stage" process [11] using a computer-controlled deposition system. In this process, the vacuum base pressure was in the 6×10^{-7} torr range. The first stage consists of depositing an $(In,Ga)_2 Se_3$ precursor layer at a substrate temperature (T_{sub}) of ~ 400°C. The precursor layer, in the second stage, is exposed to Cu and Se fluxes to form slightly Cu-rich CIGS at $T_{sub} = 585$°C. In this stage, a drop in T_{sub} occurs due to the formation of a liquid-phase Cu_{2-x} Se that encourages grain growth [12,13]. In the third stage, a small amount of In, Ga, and Se are added to the Cu-rich CIGS layer to form Cu-poor CIGS film, i.e., Cu $(In,Ga) Se_2$. Under continued Se flux, the sample is controllably cooled down to 400°C, after which the Se flux is turned off and the sample is allowed to cool down naturally to room temperature. The device fabrication was performed by chemical-bath deposition of about 500 Å CdS followed by 500 Å intrinsic ZnO and 3500 Å Al-doped ZnO using RF sputtering. Grids of Ni/Al were applied as a front contact. The performance of these devices was evaluated under standard conditions of 1000 W/m^2 and 25°C.

The chemical composition of the as-grown CIGS films was determined using electron-probe microanalysis (EPMA). The morphology of both the Mo-coated SLG and the as-grown CIGS films was examined using high-resolution, field-emission scanning electron microscopy (FESEM). X-ray diffraction (XRD) was used to examine the film microstructure such as preferred orientation and the residual intrinsic stress.

Results and Discussion

Mo Thin Films

Using XRD techniques ($\sin^2\Psi$ method [2]) and standard software provided by Scintag for data evaluation, residual intrinsic stress for the Mo films was determined as a function of Ar pressure. Figure 1 shows in-plane stresses σ_{11} (the parallel component, where the Euler angle $\varphi = 0°$). It is clear that the stress of the films sputtered at low Ar pressure is compressive. At about 1 mtorr a transition of the stress from compressive to tensile is evident. The tensile stress reaches its maximum value at about 5 mtorr, then starts decreasing as the working gas pressure increases. The bulk resistance increases with increasing working gas pressure, as shown in Figure 2. The high tensile stress and its subsequent reduction with increasing working gas pressure will be discussed in a later section.

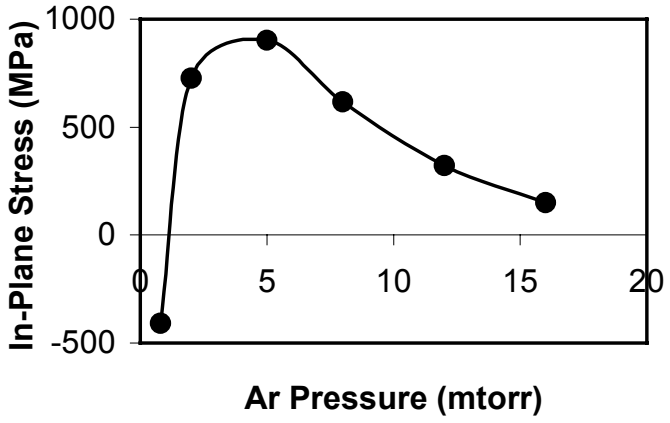

Fig.1 In-plane stresses vs. Ar pressure. Negative values represent compressive stress whereas positive values represent tensile stress.

Using the $K\alpha_1$ line of Cu, the X-ray $\theta/2\theta$ diffraction pattern revealed that all Mo films exhibit a strong < 110 > texture parallel to the growth direction. This is expected for bcc lattices such as Mo, because of the minimum surface energy

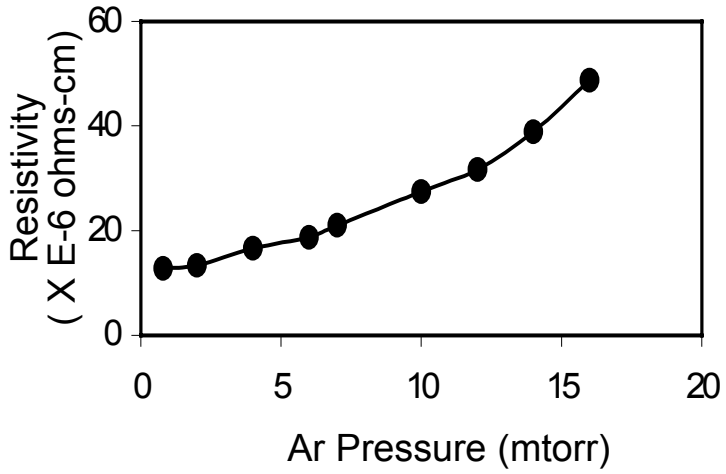

Fig.2. Resistivity as a function of Ar pressure.

associated with {110} planes and their very dense packing [4]. The effect of sputtering pressure on film microstructure is illustrated by the SEM images shown in Figures 3a–f. The cross-sectional SEM images show that all Mo films are characterized by columnar morphology. At 0.8 mtorr, where the film is under compressive stress, the columns are tightly packed. The planar view reveals that this film had a densely packed, small-grain microstructure with closed grain-boundaries. No strong evidence of the presence of voids was obtained. This microstructure was expected at very low sputtering pressures due to the peening effect caused by the Mo energetic particles [5,14]. Films deposited at 5 mtorr, where the maximum tensile stress occurred, had porous and fibrous grains with fine valleys. The morphology consisted of elongated grains with open grain-boundary structure of tapered crystallites with domed tops [6]. The cross-sectional view of this film reveals that this film had closed intercolumnar gaps. The columns are about 130 nm in width. However, film deposited beyond the tensile stress maximum at 8 mtorr had an open columnar structure. It consists of free-standing columns with widths of about 75 nm, because of the increasing amount of column boundary voids. The planar view reveals that the fibrous grain structure had large, aligned, elongated grains with the presence of microcracks.

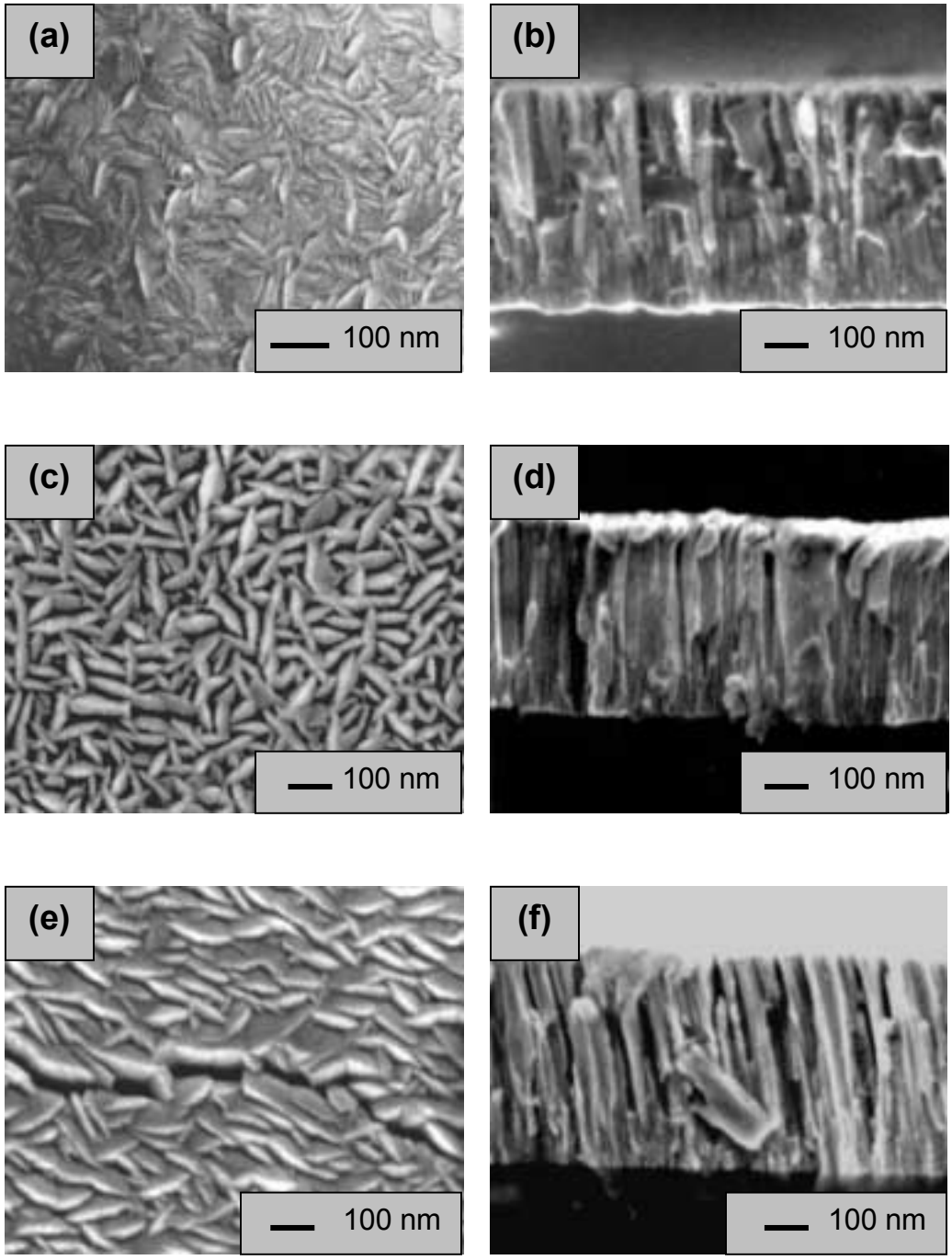

Fig. 3. SEM planar and cross-sectional views for Mo films sputtered (a and b) at 0.8 mtorr, (c and d) at 5 mtorr, and (e and f) at 8 mtorr.

As mentioned earlier, the SLG substrate temperature T was increasing during the sputtering process from about room temperature to about 400 K. Consequently, the ratio of T/T_m also was increasing from 0.1 to 0.14, where T_m is the molybdenum melting point of 2895 K. According to Thornton's diagram [15], we cannot expect a uniform microstructure, but rather, a substructure of zone I at the film/substrate interface followed by another substructure of zone T, where zone I is defined by a ratio of $T/T_m \leq 0.1$ for bcc materials. This can be verified by the presence of the microcolumnar structure at the film/substrate interface.

One way to explain the increase and then decrease in the tensile stress with increasing working gas pressure is to correlate it with the differences in the morphology of the films. It had been found that the decrease in the tensile stress, with increasing the sputtering pressure and decreasing the particles' energy, is caused by a microstructure transformation from a very compact atomic network of small "closed voids" into a porous microcolumnar with "large voids" network combined with an increase in the intercolumnar gaps [16]. The stress relaxation at low working gas pressures had been qualitatively explained by the loss in the interatomic forces acting on the grain boundary produced by the film porosity [5]. Therefore, the maximum tensile stress (at 5 mtorr) can be considered as a net result of the combination of stress build-up by intracolumnar voids and stress relaxation caused by porosity that causes a loss in intercolumnar coupling at column boundaries. Also, the tensile stress reduction or relaxation can be attributed to the increase in the dimensions of the columns and the amount of column boundary voids at high working gas pressure [2].

CIGS Thin Films

CIGS films were subsequently deposited on the Mo films, which were grown with different sputtering pressure conditions, using fixed physical vapor deposition rates for Cu, In, Ga, and Se. The chemical compositions for some selected CIGS films are summarized in Table 1. All samples had similar compositions and similar Ga/(In + Ga) atomic ratios of about 0.3.

Table 1. Samples chemical composition in at % and Ga/(In + Ga) ratios

Sample ID	P_{Ar} mtorr	Cu	In	Ga	Se	Ga/(In + Ga)
a	0.8	24.11	17.03	7.27	51.58	0.299
b	2	21.43	18.11	7.20	53.26	0.284
c	5	23.76	18.09	6.38	51.77	0.261
d	8	23.83	17.94	7.45	50.77	0.293
e	12	24.42	17.78	7.31	50.61	0.291
f	16	24.84	17.01	7.72	50.44	0.312

Figure 4 shows the X-ray $\theta/2\theta$ diffraction patterns for some selected CIGS films described in Table 1. CIGS films exhibit a (220/204) preferred orientation, where the compressive stress and stress relaxation regions are located for the

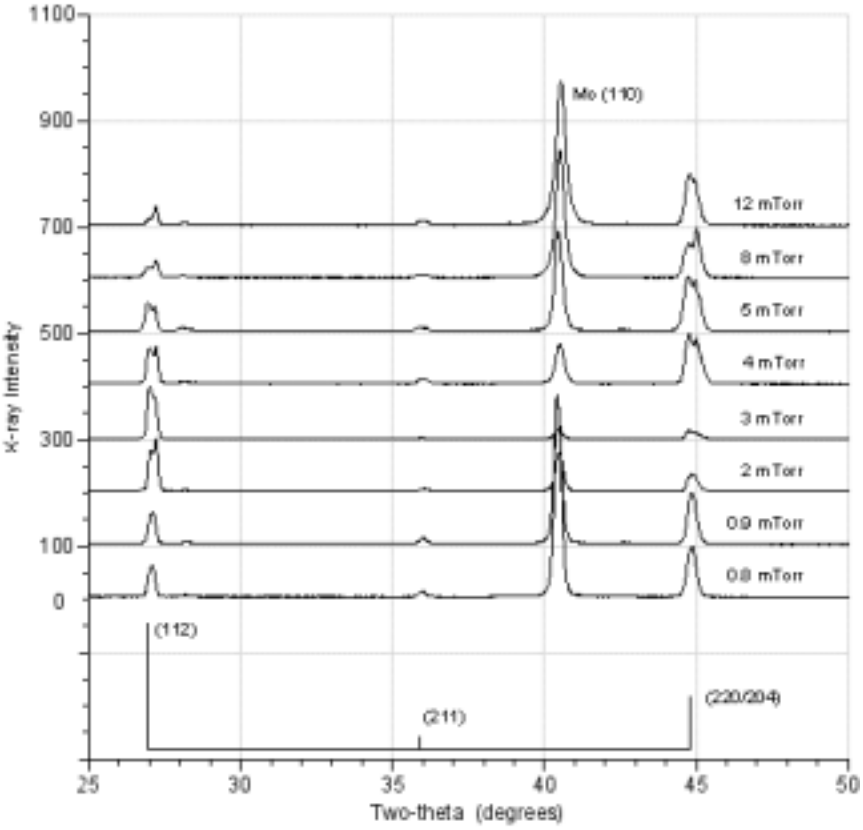

Fig.4. XRD data for CIGS films reflects the 220/204 preferred orientation in the compressive and stress relaxation regions for the Mo films. The stick diagram for randomly-oriented powder CIGS sample is shown with the highest three Bragg peaks (JCPDS card 35-1102).

Mo substrate sputtered films, as shown in Figure 1. Considering the expected intensities (stick diagram shown in Figure 4) from a randomly oriented powder sample (JCPDS card 35-1102), it is clear that CIGS films deposited on the Mo substrates sputtered in the stress build-up region show a random orientation where the intensity of (112) reflection is the highest.

The SEM investigations show that the morphology of the CIGS films varies from one sample to another in spite of the fixed deposition conditions for the CIGS films, such as the deposition rate, and the substrate temperature. The cross-sectional and planar views of the morphology of sample a, which was deposited on the Mo film grown at 0.8 mtorr (compressive stress condition), are shown in Figure 5a-b. This CIGS film surface exhibits two microstructural features. One surface is the lamellar-type microstructure, where the layers are positioned at various angles to the substrate [11,17,18], and the other surface consists of tightly packed, sharp-faceted grains of < 1 μm in width. It has been reported [10] that the lamellar-type layered structure is actually a mixed lamellar intergrowth due to the presence of In_2Se_3 and γ phases, represented on the

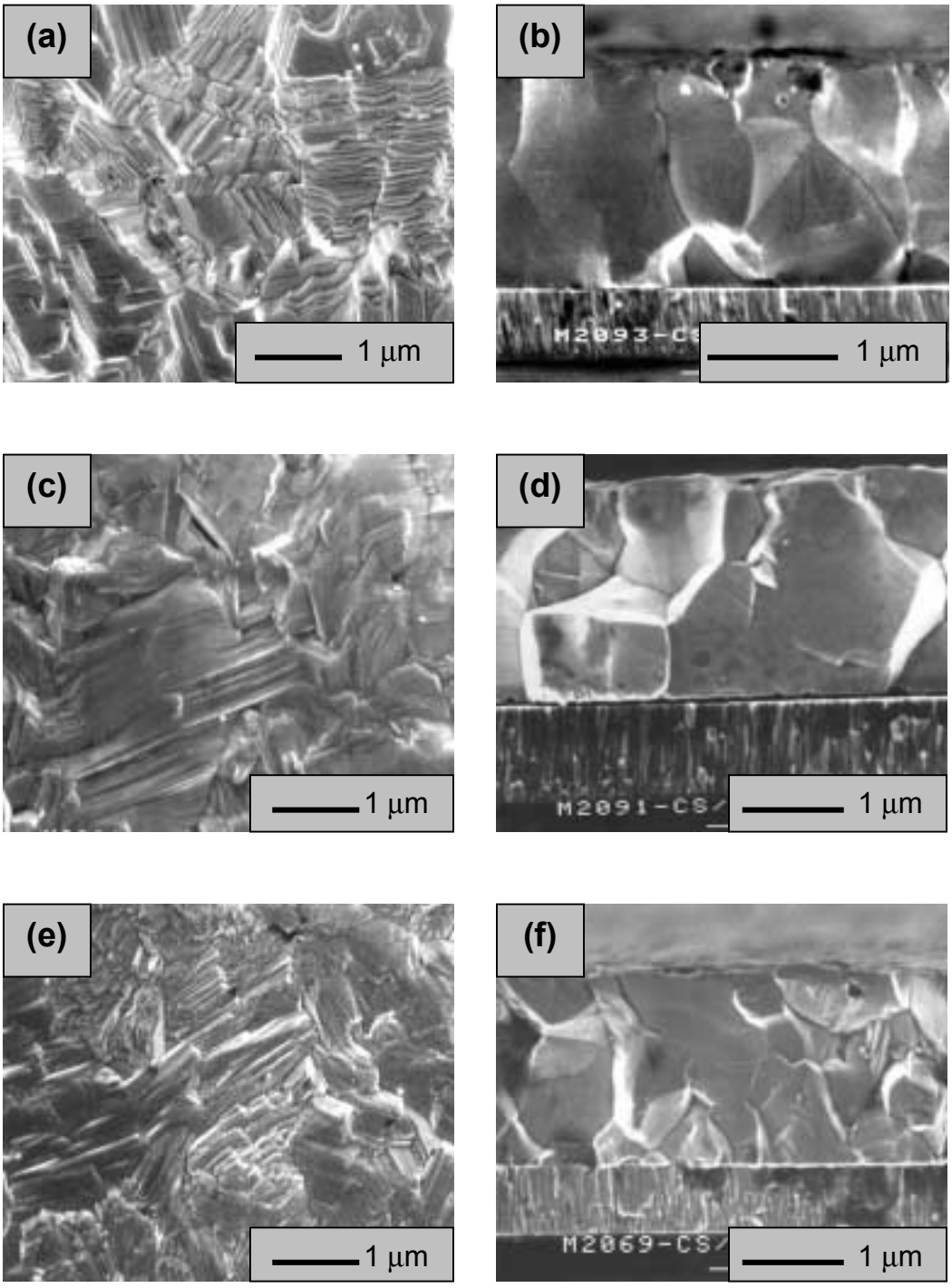

Fig. 5. SEM planar and cross-sectional views for CIGS films deposited on Mo sputtered films (a and b) at 0.8 mtorr, (c and d) at 5 mtorr, and (e and f) at 8 mtorr.

Cu_2Se-In_2Se_3 pseudo-binary phase diagram. On the other hand, the morphology of sample c, which was deposited on Mo film grown at 5 mtorr (maximum tensile stress condition), shown in Figure 5c–d, has less faceted, very dense, and smooth grains. The grain were large in size. Grains as large as 2.5 μm were observed. Sample d, which was deposited on a Mo film grown at 8 mtorr (stress relaxation condition), regains a rough surface with more sharp and faceted large grains, as shown in Figure 5e–f. The porosity of the Mo films with their open-grain structure assists in Na diffusion from the SLG substrate into the absorber CIGS layer during the deposition in the second stage at the high temperature of about 585°C. Na diffusion is advantageous during the CIGS growth because it leads to a better film morphology and a higher conductivity. Further, its incorporation induces changes in the defect distribution of the absorber films [19,20].

Table 2 represents the average performance of 24 solar cells fabricated on each sample represented in Table 1, without antireflective coating and with total area of 0.43 cm^2/cell. The cell corresponding to sample c has the highest average efficiency of 15.99%. It appears that the combined structural properties of the open–grain structure for the Mo-sputtered film and the smooth CIGS absorber film are correlated with the best average V_{oc} of 0.671 mV and average J_{sc} of 32.57 mA/cm^2.

Table 2. Average results for solar cells for the selected samples

Sample ID	P_{Ar} (mtorr)	V_{oc} (mV)	J_{sc} (mA/cm^2)	FF (%)	η (%)
a	0.8	0.624	30.85	74.64	14.36
b	2	0.658	31.71	73.10	15.25
c	5	0.671	32.57	73.20	15.99
d	8	0.677	32.14	70.64	15.77
e	12	0.643	31.24	73.63	14.79
f	16	0.574	30.64	69.64	12.35

Conclusions

This work points out the relation between the intrinsic stress and microstructure of sputtered Mo films as a function of working Ar gas pressure. A typical transition curve from compressive to tensile was observed. The microstructure of the compressively stressed films consists of tightly packed columns with closed grain-boundary structure, whereas films under tensile stress become porous with opened grain-boundary structure, and the porosity increases as the working gas pressure increases. Using our 3-stage process, CIGS films were deposited on the Mo films. CIGS films deposited on the Mo substrate in the tensile build-up region exhibit a random orientation. On the other hand, for the Mo films in the compressive-stress and the stress-relaxation regions, CIGS films exhibit (220/204) preferred orientation. The surfaces of all CIGS films show the

lamellar microstructure. The microstructure differences may be attributed to the presence of two or more of the very In-rich phases found elsewhere [11]. The highest-efficiency device was obtained for the Mo substrates sputtered at a pressure where the maximum value of the tensile stress is located.

Acknowledgments

The authors wish to thank James Keane and James Dolan for their technical support. This work was supported by a scholarship from the UAE government and the U.S. Department of Energy under Contract No. DE-AC36-99-GO10337.

References

[1] K. Granath, A. Rockett, M. Bodegard, C. Nender, and L. Stolt, Mechanical Issues of Mo Back Contacts for Cu(In,Ga)Se_2 Devices, 13th European Photovoltaic Solar Energy Conference, Nice, France, H.S. Stephens & Associates, Felmersham (1995).

[2] T. J. Vink, M. A. J. Somers, J. L. C. Daams, and A. G. Dirks, Stress, Strain, and Microstructure of Sputter-Deposited Mo Thin Films, J. Appl. Phys. **70,** 4301 (1991).

[3] T. J. Vink, and J. B. D. van Zon, Stress in Sputtered Mo Thin Films: The Effect of the Discharge Voltage, J. Vac. Sci. Technol. **A9,** 124, (1991).

[4] T. P. Drusedau, F. Klabunde, P. Veit, and T. Hempel, Investigations on Microstructure, Surface Topography, and Growth Process of Sputtered Molybdenum Showing Texture Turnover, Phys. Stat. Sol. **161,** 167, (1997).

[5] M. Itoh, M. Hori, and S. Nadahara, The Origin of Stress in Sputter-Deposited Tungsten Films for X-Ray Masks, J. Vac. Sci. Technol. **B9 ,** 149, (1991).

[6] T. Yamaguchi and R. Miyagawa, Effects of Oxygen on the Properties of Sputtered Molybdenum Thin Films, Jpn. J. Appl. Phys. **30,** no. 9 A, 2069 (1991).

[7] Richard H. Bube, Photovoltaic Materials, Imperial College Press, London, 1998, pp 190.

[8] T. Dullweber, G. Hanna, W. Shams-Kolahi, A. Schwartzlander, M. A. Contreras, R. Noufi, and H. W. Schock, Study of the Effect of Gallium Grading in Cu(In,Ga)Se_2, Thin Solid Films **361-362,** 478, (2000).

[9] M.A. Contreras, H. Wiesner, J. Tuttle, K. Ramanathan, and R. Noufi, *"Issues on the Chalcopyrite/Defect Junction Model for High Efficiency Cu(In,Ga)Se_2 Solar Cells"*, Technical Digest of the International PVSEC-9, Miyazaki, Japan, 1996, pp. 127-130.

[10] M. A. Contreras, B. Egaas, K. Ramanathan, J. Hiltner, A. Swartzlander, F. Hasoon, R. Noufi, Progress Toward 20% Efficiency in Cu(In,Ga)Se_2 Ploycrystalline Thin-Film Solar Cells, Prog. Photovolt. Res. Appl. **7,** 311, (1999).

[11] F. S. Hasoon, Y. Yan, H. Althani, K. M. Jones, J. Alleman, M. M. Al-Jassim, and R. Noufi, Microstructural Properties of Cu(In,Ga)Se_2 Thin Films Used in High-Efficiency Devices, Thin Solid Films, in press.

[12] U. C. Bohnke and G. Kuhn, Phase Relations in the Ternary System Cu-In-Se, J. of Materials Science **22**,1635 (1987).

[13] J. C. Mikkelsen, Jr., Ternary Phase Relations of the Chalcopyrite Compound CuGaSe, J. of Electronic Materials **10,** 541 (1981).

[14] H. Windischmann, An Intrinsic Stress Scaling Law for Polycrystalline Thin Films Prepared by Ion Beam Sputtering, J. Appl. Phys. **62,** 1800, (1987).

[15] J. A. Thornton, High Rate Thick Film Growth*,* Ann. Rev. Mater. Sci. **7,** 239 (1977).

[16] K. H. Muller, Stress and Microstructure of Sputter-Deposited Thin Films: Molecular Dynamics Investigation, J. Appl. Phys. **62,** 1796, (1987).

[17] S. Nishiwaki, T. Satoh, S. Hayashi, Y. Hashimoto, T. Negami, and T. Wada, Preparation of Cu(In,Ga)Se_2 Thin Films From In-Ga-Se Precursors for High-Efficiency Solar Cells, J. Mater. Res. **14**, 4514, (1999).

[18] S. Cattarin, C. Pagura, L. Armelao, R. Bertoncello, and N. Dietz, Surface Characterization of $CuInS_2$ with Lamellar Morphology, J. Electrochem. Soc. **142,** 2818, (1995).

[19] U. Rau and H. W. Schock, Electronic Properties of Cu(In,Ga)Se_2 Heterojunction Solar Cells-Recent Achievements, Current Understanding, and Future Challenges, Appl. Phys. **A 69,** 131, (1999).

[20] D. Braunger, D. Hariskos, G. Bilger, U. Rau, and H. W. Schock, Influence of Sodium on the Growth of Polycrystalline Cu(In,Ga)Se_2 Thin Films, Thin Solid Films **361-362,** 161, (2000).

REPORT DOCUMENTATION PAGE

Form Approved
OMB NO. 0704-0188

1. AGENCY USE ONLY (Leave blank)	2. REPORT DATE	3. REPORT TYPE AND DATES COVERED
	January 2001	Conference Paper

4. TITLE AND SUBTITLE
The Deposition and Characterization of Mo/CuInGaSe$_2$/CdS/ZnO Solar Cells

5. FUNDING NUMBERS
C:
TA: PVP1.4301

6. AUTHOR(S)
H.A. Al-Thani, F.S. Hasoon, J.L. Alleman, M.M. Al-Jassim, D.L. Williamson

7. PERFORMING ORGANIZATION NAME(S) AND ADDRESS(ES)
National Renewable Energy Laboratory
1617 Cole Blvd.
Golden, CO 80401-3393

8. PERFORMING ORGANIZATION REPORT NUMBER
NREL/CP-520-29641

9. SPONSORING/MONITORING AGENCY NAME(S) AND ADDRESS(ES)

10. SPONSORING/MONITORING AGENCY REPORT NUMBER

11. SUPPLEMENTARY NOTES

12a. DISTRIBUTION/AVAILABILITY STATEMENT
National Technical Information Service
U.S. Department of Commerce
5285 Port Royal Road
Springfield, VA 22161

12b. DISTRIBUTION CODE

13. ABSTRACT *(Maximum 200 words)*

Mo thin films were deposited on sodalime glass (SLG) substrates using direct-current planar magnetron sputtering, with a sputtering power density of 1.18 W/cm^2. The working gas (Ar) pressure was varied from 0.6 mtorr to 16 mtorr to gain a better understanding of the effect of sputtering pressure on the morphology and microstructure of the Mo. Thin films of Cu(In,Ga)Se$_2$ (CIGS) were deposited on the Mo-coated glass using the 3-stage coevaporation process. The morphology of both the Mo-coated SLG and the CIGS thin films grown on it was examined using high-resolution scanning electron microscopy. The film microstructure, such as the preferred orientation, and the residual intrinsic stress were examined by X-ray diffraction.

14. SUBJECT TERMS
photovoltaics; Mo; Cu(In,Ga)Se$_2$; CIGS; 3-stage process; intrinsic stress; microstructure

15. NUMBER OF PAGES

16. PRICE CODE

17. SECURITY CLASSIFICATION OF REPORT	18. SECURITY CLASSIFICATION OF THIS PAGE	19. SECURITY CLASSIFICATION OF ABSTRACT	20. LIMITATION OF ABSTRACT
Unclassified	Unclassified	Unclassified	UL